

Supporting Information

High-sensitivity X-ray Detectors Based on Solution-grown Caesium Lead Bromine Single Crystals

Hongjian Zhang, Fangbao Wang, Yufei Lu, Qihao Sun, Yadong Xu*, Binbin Zhang*, Wanqi Jie, Mercouri. G. Kanatzidis

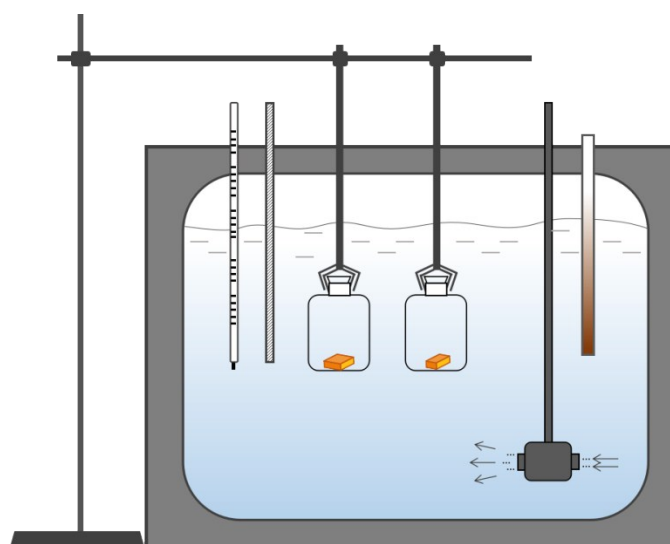


Figure S1. The schematic diagram of crystal growth equipment of ITC method.

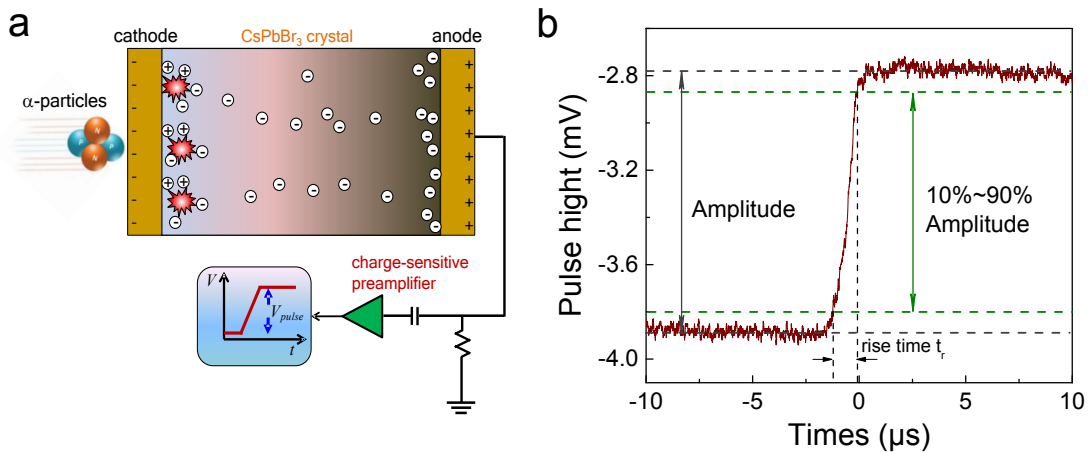


Figure S2. α -particle-induced pulse shape rise time analysis. a) Diagram of the transport process of electrons and holes in CsPbBr_3 crystal illuminated under α particles and the signal measurement setup. b) A typical pulse high waveform under 10 V bias from the preamplifier, and the rise time is defined as the span of 10%~90% amplitude.

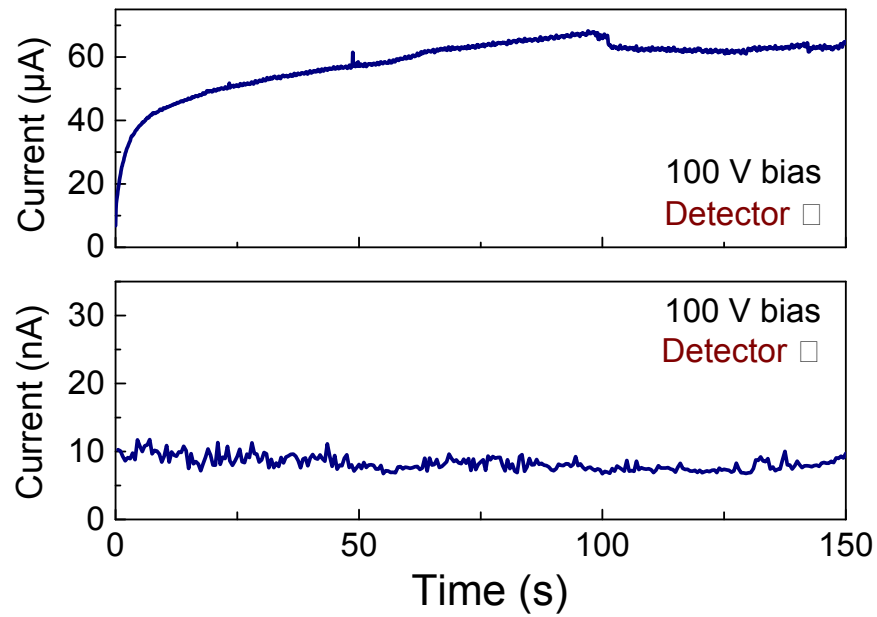


Figure S3. Dark current variation with time under 100 V positive bias for detector I and detector II.

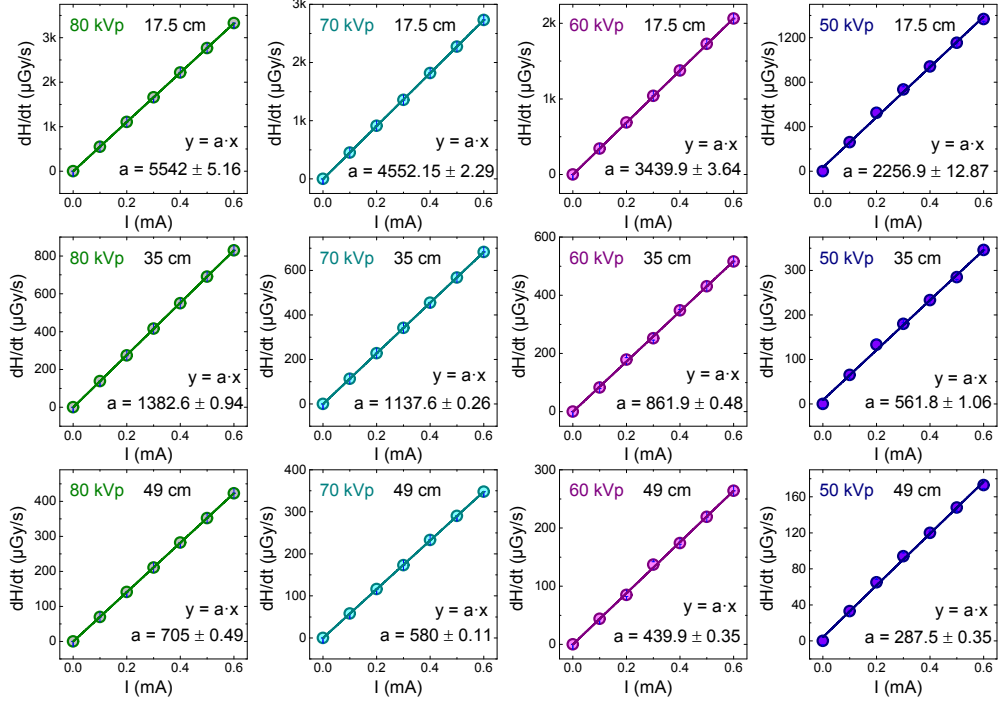


Figure S4. The fitting results of dose rates as functions of tube currents under the tube voltage of 80 kV, 70 kV, 60 kV, 50 kV, and the distance (from the sample to the source) of 17.5 cm, 35 cm, and 49 cm respectively, calibrated by ion chamber dosimeter and thermoluminescence meters.

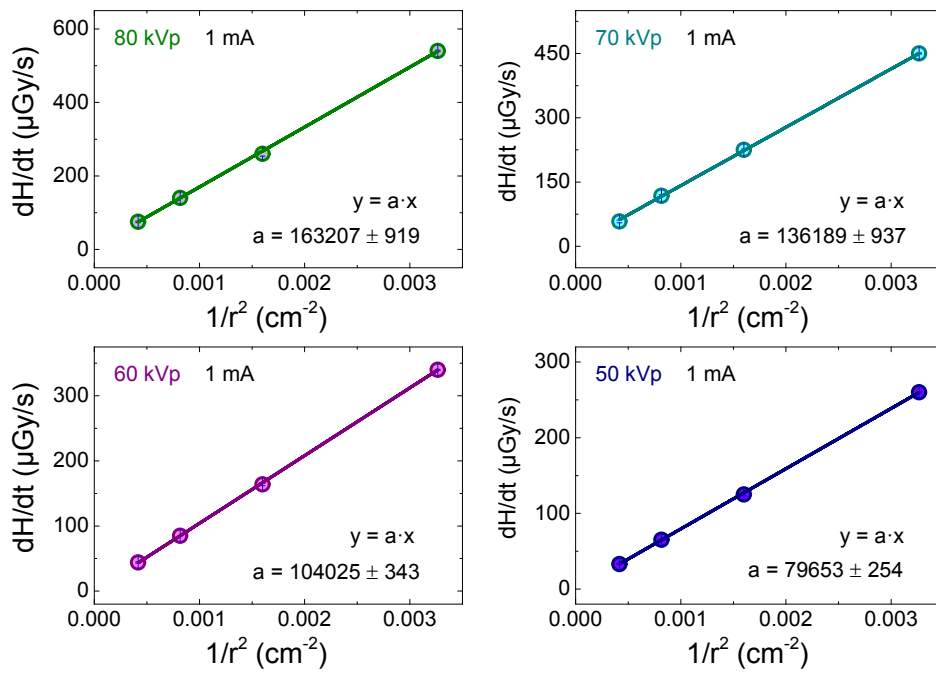


Figure S5. The fitting results of dose rates as functions of $1/r^2$ (r is the distance from the sample to the source), under the 80 kVp, 70 kVp, 60 kVp and 50 kVp X-ray, respectively.

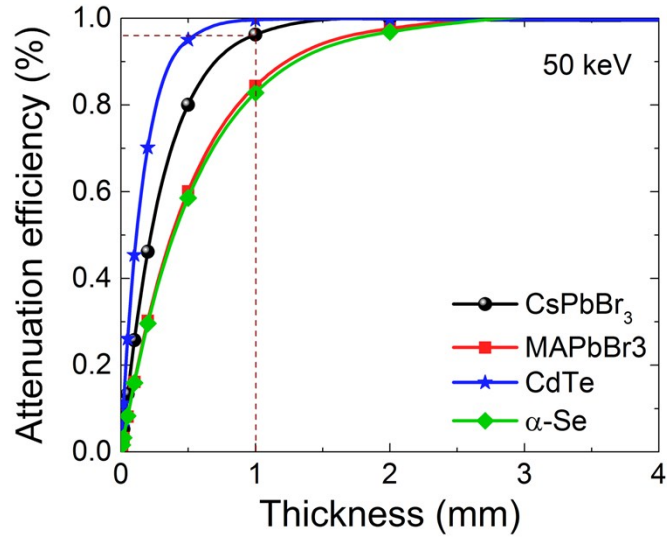
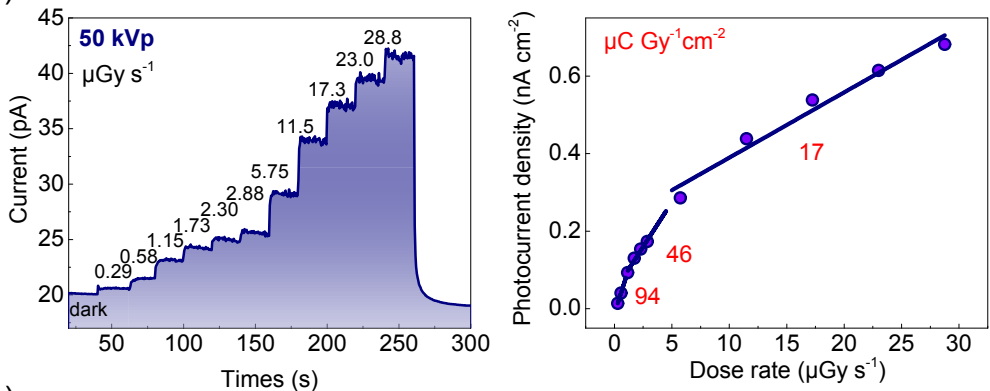
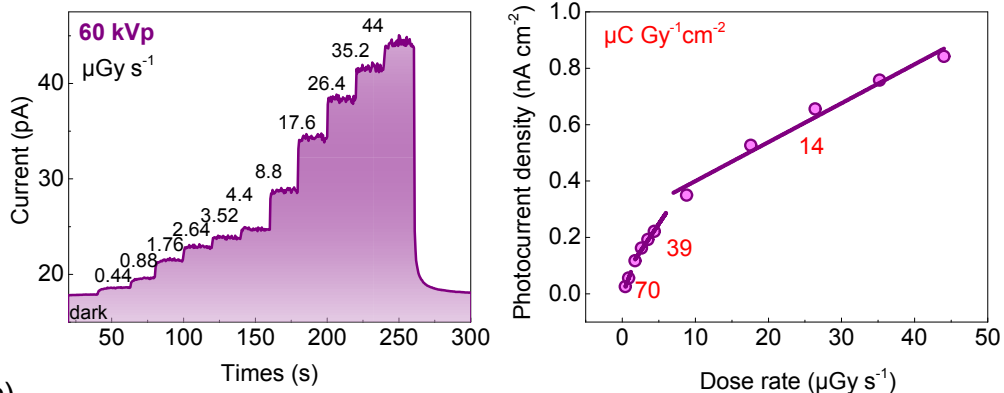


Figure S6. Attenuation efficiency of CsPbBr_3 and some representative materials to 50 keV X-ray photons versus thickness.

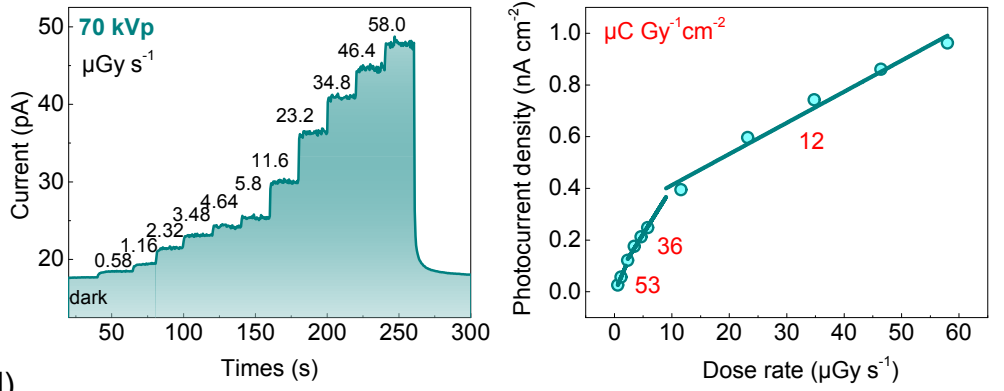
(a)



(b)



(c)



(d)

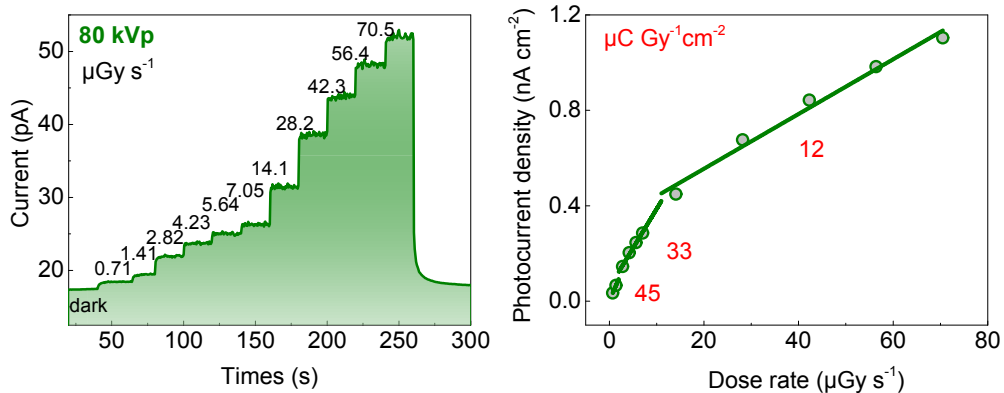


Figure S7. The X-ray response and the fitted sensitivity of a) 50 kVp, b) 60 kVp, c) 70 kVp and d) 80 kVp X-ray under the electric field strength of 1 V/mm on detector I.

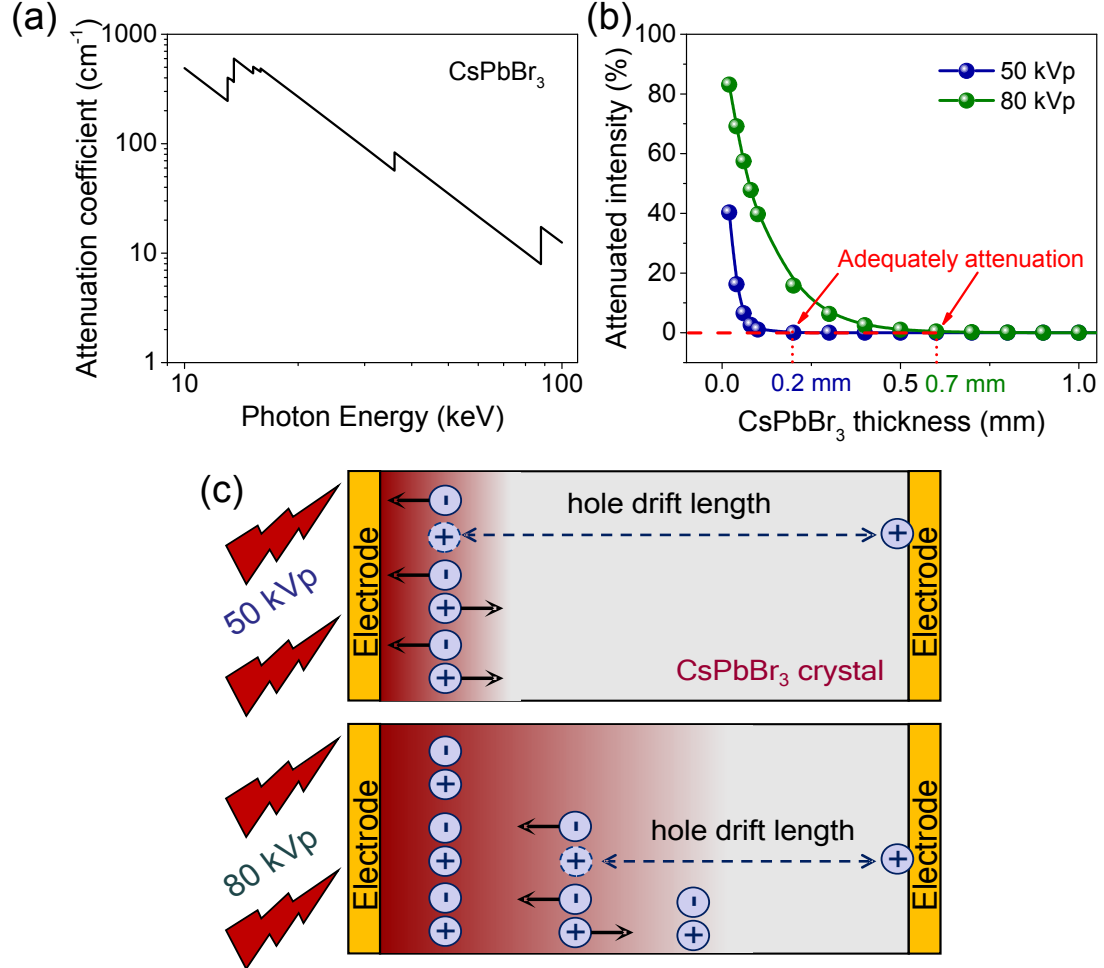


Figure S8. Attenuation variations between 50 and 80 kVp X-ray in CsPbBr_3 samples. a) Attenuation coefficient for CsPbBr_3 in the 10-100 keV energy range. b) Attenuated intensity of 50 and 80 kVp X-ray in CsPbBr_3 . The red dash line indicates adequately attenuation, and the corresponding sample thickness are 0.2 mm and 0.7 mm for 50 and 80 kVp respectively. c) The schematic variations of hole drift length for 50 and 80 kVp X-ray detection.

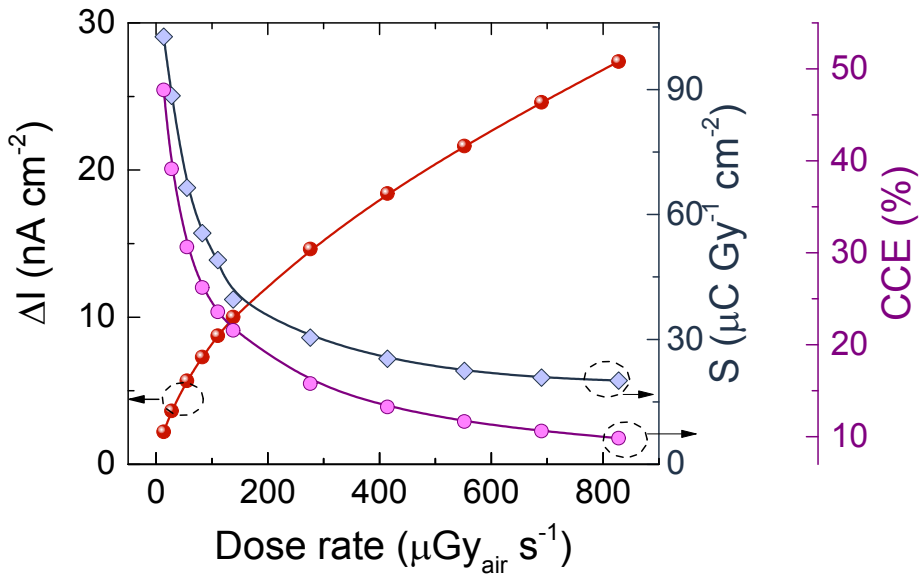


Figure S9. The variation of gained photocurrent density, sensitivity, and charge collection efficiency (CCE) with dose rate under 80 kVp X-ray and 1 V/mm electric field for detector I.

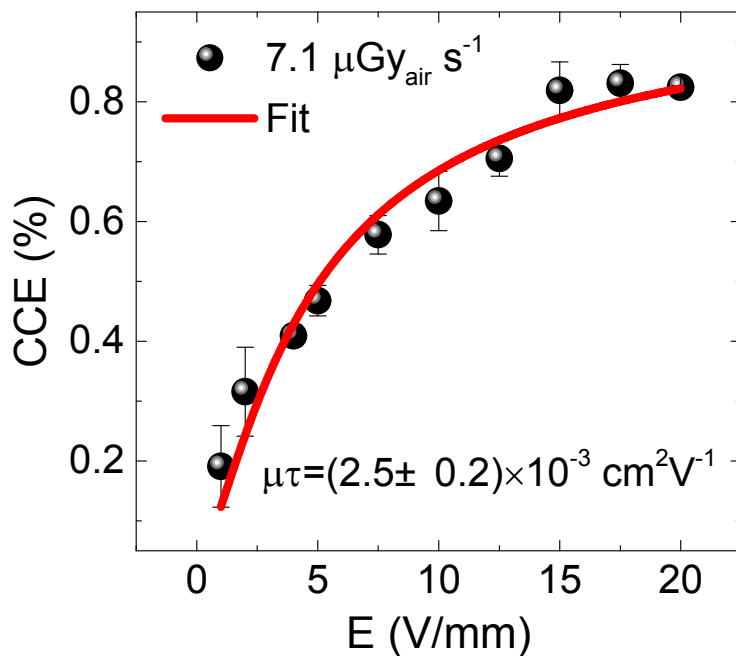


Figure S10. By fitting the electric field dependent charge collection efficiency using single carrier Hatch function, the mobility-lifetime product was obtained as $(2.5 \pm 0.2) \times 10^{-3} \text{ cm}^2 \text{V}^{-1}$ under the X-ray dose rate of $7.1 \text{ CGy}^{-1} \text{s}^{-1}$.